

First-Principles Study on the MAX Phases $Ti_{n+1}GaN_n$ ($n = 1, 2, \text{ and } 3$)

GOKHAN SURUCU,^{1,2,6} KEMAL COLAKOGLU,³ ENGIN DELIGOZ,^{4,7}
and NURETTIN KOROZLU⁵

1.—Department of Electrics and Energy, Ahi Evran University, 40100 Kirsehir, Turkey. 2.—Photonics Application and Research Center, Gazi University, 06500 Ankara, Turkey. 3.—Department of Physics, Gazi University, 06500 Ankara, Turkey. 4.—Department of Physics, Aksaray University, 68100 Aksaray, Turkey. 5.—Department of Nanoscience and Nanotechnology, Mehmet Akif Ersoy University, 15000 Burdur, Turkey. 6.—e-mail: g_surucu@yahoo.com. 7.—e-mail: edeligoz@yahoo.com

We have performed first-principles density functional theory calculations within generalized-gradient approximation to obtain the structural, mechanical, electronic, and dynamic properties of $Ti_{n+1}GaN_n$ compounds. In order to examine the stability of these compounds, formation enthalpies, single-crystal elastic constants, and phonon dispersion curves were calculated. We show that all compounds are stable, while $\alpha-Ti_4GaN_3$ is the most stable. The density of states calculations also demonstrate that all of the compounds are metallic. Additionally, bonding nature and related characteristics such as Mulliken atomic charges and bond overlap populations were investigated. Furthermore, thermodynamic properties were calculated by means of phonon dispersion curves. The results are compared in this work with available experimental values and theoretical calculations.

Key words: MAX phases, electronic properties, phonons, mechanical properties, first-principles

INTRODUCTION

The $M_{n+1}AX_n$ phases (where M, A, and X are a transition metal, A-group element, and either C or N, respectively) have attracted considerable attention due to their promising properties which establish connections between metallic and ceramic properties, such as high strength and stiffness at high temperatures, resistance to oxidation and thermal shock, good damage tolerance, good corrosion resistance, and good thermal and electrical conduction.^{1–3} Therefore, $M_{n+1}AX_n$ phases are promising materials for many applications such as rotating electrical contacts and bearings, heating elements, nozzles, heat exchangers, and tools for depressing, among many others.⁴

Several physical properties of $M_{n+1}AX_n$ phases have been studied by different researchers. For

instance, Dahlqvist et al. investigated the phase stability of MAX ($M = Sc, Ti, V, Cr, \text{ or } Mn, A = Al, \text{ and } X = C \text{ or } N$).⁵ They reported that a maximum stability is reached around V as a transition metal, while for nitrogen, the maximum stability is reached for Ti for carbon-containing MAX phases. In addition, Keast et al. predicted the stability of an $M_{n+1}AX_n$ system containing α - and β -phases for different values of n .⁶ Their results suggest that Ti_2SiC , Ti_2SiN , and Ti_3AlN_2 have the potential to be synthesized as metastable compounds.

M_2GaN (M is either Ti, V, or Cr) was investigated systematically to identify trends for structural, electronic, and elastic properties by Bouhemadou.⁷ Yang et al. performed comprehensive investigations on the compressive and electronic properties of Ti_2GaN and applied high pressure to the compound up to 1000 GPa.² On the other hand, Manoun et al. measured the pressure dependency of the structural and mechanical properties of Gallium-containing polycrystalline Ti_2GaN and Cr_2GaC as

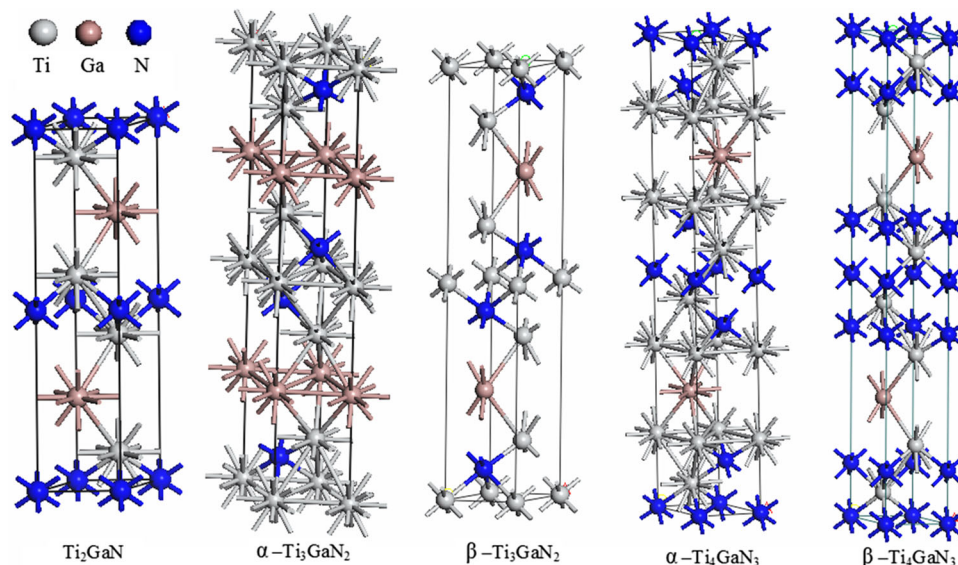


Fig. 1. Crystal structures of $Ti_{n+1}GaN_n$ ($n = 1, 2,$ and 3) compounds.

experimental MAX phases.⁸ Shein and Ivanovskii systematically studied the trends in structural and electronic properties, as well as the relative stability of a representative group of very recently discovered materials prepared from de-intercalated MAX phases.⁹ Furthermore, as an important result, they reported that $M_{n+1}AX_n$ phases can be used as graphene-like structures. Systematic experimental studies of MAX-phase solid solutions to elucidate the role of chemistry on phase stability and properties were carried out by Eklund et al.¹⁰

Despite a large number of theoretical and experimental studies devoted to the M_2AX phase, to our best knowledge, until now no other systematic results have been reported on the mechanical, electronic, and dynamic properties of $Ti_{n+1}GaN_n$ compounds. Hence, we report here the structural, mechanical, electronic, and dynamic properties of $Ti_{n+1}GaN_n$ compounds as investigated by first-principles calculations in our study. After well-converged geometry optimizations, we tested the energetic, mechanic, and dynamic stabilities of the compounds, and then compared the results to some experimental data and to those of similar compounds with the same structure.

CALCULATION METHOD

First-principles density functional plane wave calculations were performed using the CASTEP package under generalized gradient approximation (GGA-PW91).^{11,12} To define interactions between electrons and ion cores, norm-conserving pseudopotentials were used.^{13,14} The wave functions were expanded in plane waves up to a kinetic-energy cutoff of 880 eV. The numerical integration over the Brillouin zone was performed using a $14 \times 14 \times 4$, $10 \times 10 \times 2$, $14 \times 14 \times 2$, $10 \times 10 \times 2$ and $14 \times 14 \times 2$ Monkhorst-Pack k -point grids for Ti_2GaN ,

α - Ti_3GaN_2 , β - Ti_3GaN_2 , α - Ti_4GaN_3 , and β - Ti_4GaN_3 crystal structures, respectively.¹⁵ During the geometry optimizations, there are no restrictions on lattice parameters and atomic locations, and the structures were relaxed using the Broyden, Fletcher, Goldfarb, and Shannon (BFGS) method.¹⁶ The convergence criteria are (i) 5×10^{-6} eV/atom for total energy, (ii) 0.01 eV/Å for maximum ionic Hellmann-Feynman force, (iii) 5×10^{-4} Å for maximum ionic displacement, and (iv) 0.02 GPa for maximum stress.

RESULTS AND DISCUSSION

Structural and Electronic Properties

The $M_{n+1}AX_n$ phases crystallize in a hexagonal structure (space group P63/mmc) with two formula units per unit cell.³ Crystal structures of $Ti_{n+1}GaN_n$ ($n = 1, 2,$ and 3) compounds are formed by ceramic-like strongly bonded MX atomic layers and interleaved A layers (see Fig. 1). Structural optimizations were performed, including lattice parameters and internal coordinates. The calculated lattice parameters (a , c) and atomic positions are given in Table I.

Our results for Ti_2GaN agree well with previous theoretical and experimental reports.^{7,8} Since there are no experimental and theoretical data for the other compounds, the results for these compounds are compared to those of the compounds including A = Si and Al.⁶ The lattice parameters of α -type (β -type) compounds are smaller (higher) than those of the A = Ga case.

For $Ti_{n+1}GaN_n$ compounds, formation enthalpies were also calculated using the following common relation:

$$E_{\text{from}}^{Ti_{n+1}GaN_n} = E_{\text{total}}^{Ti_{n+1}GaN_n} - [(n+1)E_{\text{solid}}^{Ti} + E_{\text{solid}}^{Ga} + nE_{\text{solid}}^N] \quad (1)$$

Table I. The calculated equilibrium lattice parameters (a , and c in Å), atomic positions, and formation energies (ΔH_f in eV/atom) for $Ti_{n+1}GaN_n$ compounds

	a	c	Atomic positions		ΔH_f
Ti_2GaN	3.02	13.31	Ti 4f (1/3, 2/3, 0.088)	Ti 4f (1/3, 2/3, 0.092) ^c	-1.25
	3.00 ^a	13.33 ^a	Ga 2d (1/3, 2/3, 3/4)	Ti 4f (1/3, 2/3, 0.085) ^d	
	3.02 ^b	13.32 ^b	N 2a (0, 0, 0)		
	2.99 ^c	12.88 ^c			
	2.99 ^d	13.64 ^d			
$\alpha-Ti_3GaN_2$	3.01	18.21	Ti ₁ 2a (0, 0, 0)	Ti ₂ 4f (2/3, 1/3, 0.136) ^c	-1.42
	2.99 ^c	17.84 ^c	Ti ₂ 4f (2/3, 1/3, 0.130)	Ti ₂ 4f (2/3, 1/3, 0.129) ^d	
	3.00 ^c	18.49 ^d	Ga 2b (0, 0, 1/4)	N 4f (1/3, 2/3, 0.069) ^c	
			N 4f (1/3, 2/3, 0.069)	N 4f (1/3, 2/3, 0.068) ^d	
$\beta-Ti_3GaN_2$	2.99	18.47	Ti ₁ 2a (0, 0, 0)	Ti ₂ 4f (2/3, 1/3, 0.136) ^c	-1
	2.96 ^c	2.99 ^d	Ti ₂ 4f (2/3, 1/3, 0.129)	Ti ₂ 4f (2/3, 1/3, 0.128) ^d	
	2.99 ^d	18.67 ^d	Ga 2d (2/3, 1/3, 1/4)	N 4f (1/3, 2/3, 0.068) ^c	
			N 4f (1/3, 2/3, 0.068)	N 4f (1/3, 2/3, 0.067) ^d	
$\alpha-Ti_4GaN_3$	3.00	23.22	Ti ₁ 4e (0, 0, 0.155)	Ti ₁ 4e (0, 0, 0.160) ^c	-1.54
	3.00 ^c	22.58 ^c	Ti ₂ 4f(2/3, 1/3, 0.054)	Ti ₁ 4e (0, 0, 0.154) ^d	
	3.00 ^d	23.51 ^d	Ga 2c (2/3, 1/3, 1/4)	Ti ₂ 4f(2/3, 1/3, 0.055) ^c	
			N ₁ 4a (0, 0, 0)	Ti ₂ 4f(2/3, 1/3, 0.054) ^d	
			N ₂ 4f (2/3, 1/3, 0.106)	N ₂ 4f (2/3, 1/3, 0.109) ^c	
				N ₂ 4f (2/3, 1/3, 0.106) ^d	
$\beta-Ti_4GaN_3$	2.98	23.60	Ti ₁ 4f (1/3, 2/3, 0.055)	Ti ₁ 4f (1/3, 2/3, 0.055) ^c	-1.46
	2.99 ^c	22.87 ^c	Ti ₂ 4f (2/3, 1/3, 0.657)	Ti ₁ 4f (1/3, 2/3, 0.054) ^d	
	2.98 ^d	23.60 ^d	Ga 2c (1/3, 2/3, 1/4)	Ti ₂ 4f (2/3, 1/3, 0.159) ^c	
			N ₁ 2a (0, 0, 0)	Ti ₂ 4f (2/3, 1/3, 0.154) ^d	
			N ₂ 4f (2/3, 1/3, 0.110)	N ₂ 4f (2/3, 1/3, 0.107) ^c	
				N ₂ 4f (2/3, 1/3, 0.105) ^d	

^aRef. 8 experimental. ^bRef. 7 GGA-PBE. ^cRef. 6 data for Ga = Si. ^dRef. 6 data for Ga = Al.

where E_{solid}^{Ti} , E_{solid}^{Ga} and E_{solid}^N are calculated from Ti_2GaN , $\alpha-Ti_3GaN_2$, $\beta-Ti_3GaN_2$, $\alpha-Ti_4GaN_3$, and $\beta-Ti_4GaN_3$ structures, respectively. It is shown in Table I that all compounds are energetically stable due to the negative formation enthalpy values, indicating that it should be possible to synthesize the considered phases. Among the compounds, $\alpha-Ti_4GaN_3$ is relatively the most stable.

The calculated partial and total density of states (DOS) are shown in Fig. 2. It is clear that all compounds are metallic due to the fact that the DOS values differ from zero at the Fermi level. The most significant contribution to DOS comes from Ti d -states at the vicinity of the Fermi level. In addition, the delocalized bands in the energy range from -16 eV to -15 eV are dominated by an s orbital and from -15 eV to -13.5 eV they are dominated by a d orbital for all calculated compounds. Also, a strong hybridization exists between s and p orbitals that are from -9.5 eV to -7 eV, which indicates the presence of covalent interactions. A p orbital is dominant from -3 eV to -2 eV while a d orbital is dominant from -2 eV to 4 eV for all compounds.

On the other hand, DOS curves can be used to discuss the stability of the compounds by means of band filling theory.^{17,18} According to this theory; if

the numbers of bonding (anti-bonding) states increase (decrease), the stability of the material increases. Thus, the ratio W_{occ} (the width of the occupied states)/ W_b (the width of the bonding states) may give information about the stability of the material. If the value of this ratio is closer to 1.0, the stability increases. In this study, the parameters given in Table II for $Ti_{n+1}GaN_n$ suggest that W_{occ}/W_b values are very closer to 1.0. On account of this, the $Ti_{n+1}GaN_n$ compounds turn out to be stable materials.

PHONON DISPERSION CURVES

The phonon frequencies and phonon dispersion curves of $Ti_{n+1}GaN_n$ compounds were calculated using the "finite-displacement method" in the CASTEP package.¹⁹ Specifically, the phonon dispersion curves were calculated along high symmetry directions using a $2 \times 2 \times 2$ super cell. The obtained phonon dispersion curves are shown in Fig. 3. The calculated phonon frequencies in all directions and in all bands are real, demonstrating that these compounds are dynamically stable. Although there exist some works in the literature dedicated to these compounds, no experimental or theoretical works exist on the lattice dynamics for comparison with our results.

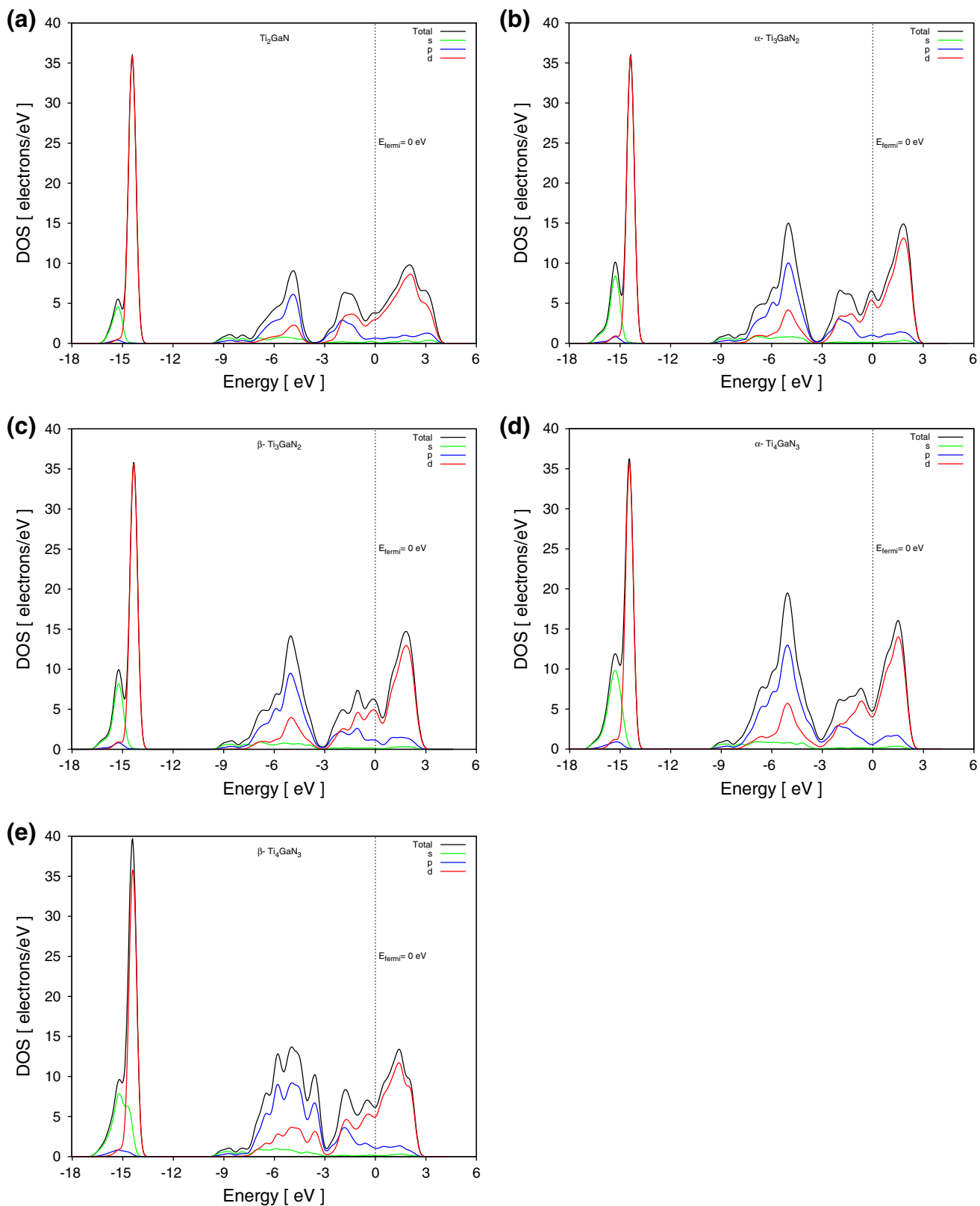


Fig. 2. Calculated partial density of states for $Ti_{n+1}GaN_n$ ($n = 1, 2,$ and 3) compounds.

Table II. The width of occupied states W_{occ} (eV) and bonding states W_b (eV) for $Ti_{n+1}GaN_n$ compounds

	W_{occ}	W_b	W_{occ}/W_b
Ti_2GaN	10.30	9.70	1.06
$\alpha-Ti_3GaN_2$	10.20	9.40	1.09
$\beta-Ti_3GaN_2$	10.10	10.30	0.99
$\alpha-Ti_4GaN_3$	10.25	10.23	1.00
$\beta-Ti_4GaN_3$	10.33	10.32	1.00

ELASTIC AND MECHANICAL PROPERTIES

The elastic constants (C_{ij}) provide information about the stability and stiffness of materials, and their first-principles calculation requires accurate methods.²⁰ In this study, the elastic constants are calculated by using both the ‘‘slope technique’’ from the phonon dispersion curves and the ‘‘stress-strain’’ method.^{21–23} For a stable hexagonal structure, there are five independent elastic constants C_{ij} (i.e. C_{11} , C_{12} , C_{13} , C_{33} , and C_{44}), and they should satisfy the well-known Born–Huang criteria for mechanical stability²⁴:

$$C_{44} > 0, C_{11} > |C_{12}|, (C_{11} + 2C_{12})C_{33} > 2C_{13}^2 \quad (2)$$

In the slope technique, the elastic modulus (C_{ij}) is obtained via the sound velocities (V) as derived from the initial slope of the acoustic phonon branches along specific high-symmetry and Christoffel’s equation.²¹ Thus, the elastic constants ($C_{11} = \rho(V_{LA}[100])^2$, $C_{33} = \rho(V_{LA}[001])^2$, $C_{66} = \rho(V_{TA}[110]_{<001>})^2$, $C_{44} = \rho(V_{TA}[110]_{<001>})^2$, and C_{13} contributes to the sound velocity only for nonpure directions, where ρ is the density) are calculated from the acoustic phonon dispersion curves. The velocity of the longitudinal acoustic (LA) phonon branches along the [100] and [001] direction, that of the two transverse acoustic (TA) branches along the [110] direction, and that of the quasi longitudinal phonon branches along the [101] direction. The sound velocities which are calculated using the acoustic phonon branches are given in Table III.

The calculated elastic constants along with the other theoretical values in literature are given in Table IV.^{2,7} It is seen that the present elastic constants of Ti_2GaN are in good agreement with the reported values.^{2,7} To the best of our knowledge, no experimental data or theoretical calculations of elastic constants for other phases have been reported. It is shown from Table IV that all compounds satisfy all the stability conditions (Eq. 2), and thus, $Ti_{n+1}GaN_n$ compounds are mechanically stable. From Table IV, it is also easily seen that $\alpha-Ti_4GaN_3$ has the largest C_{11} , C_{12} , and C_{44} . Also, C_{11} is higher than C_{33} for all considered phases, showing that the incompressibility along the [1010] and [0110] directions is stronger than that along the

[0001] direction, implying that the bonding strength along the [1010] and [0110] directions is stronger than that along the [0001] direction.²⁵

The mechanical properties, such as bulk modulus (B), Young’s modulus (E), shear modulus (G) and Poisson’s ratio (ν), which are functions of the elastic constants, are calculated by using the Voigt–Reuss–Hill approximation, and are listed in Table V.^{22,26}

The bulk modulus indicates the resistance to fracture, while the shear modulus indicates the resistance to plastic deformation. $\alpha-Ti_4GaN_3$ has the highest bulk and shear moduli. If the value of E increases, the covalent nature of the material also increases.²⁷ Therefore, the covalent character of $\alpha-Ti_4GaN_3$ is more dominant than that of other phases. Furthermore, Young’s modulus provides a measure of the stiffness of the solid.²⁸ The highest E value occurs for $\beta-Ti_4GaN_3$ among the other phases, implying that it is stiffer as compared to other phases.

We have also predicted other mechanical properties such as brittleness and ductility, as the B/G ratio can be used to predict the brittle or ductile behavior of materials. According to the Pugh criterion (B/G), a material is brittle (ductile) if the B/G ratio is less (higher) than 1.75. The present values of B/G for $Ti_{n+1}GaN_n$ compounds are less than 1.75.²⁹ Hence, these materials will behave in a brittle manner. The Ti_2GaN is the most brittle in these phases with the lowest Pugh value. Furthermore, the value of the Poisson’s ratio is small ($\nu = 0.1$) for covalent materials, whereas a typical value of ν is 0.25 for ionic materials.³⁰ From Table V, it can be seen that the calculated Poisson’s ratio values approach 0.22. Thus, it can be expected that ionic nature of these materials is high. However, $\alpha-Ti_4GaN_3$ has the smallest Poisson’s ratio, where this implies the covalent nature of the compound, and agrees with the high stability and high mechanical properties mentioned above.

Hardness is another important mechanical property of the materials and it can be theoretically calculated through different methods. A similar semi-empirical method was developed by Chen et al.³¹ In this method, hardness of a given material that should be related to bulk and shear moduli can be calculated as;

$$H_V = 2(k^2G)^{0.585} - 3 \quad (3)$$

where $k = G/B$ is Pugh’s modulus ratio. The calculated hardness values are given in Table V. According to Table V, these compounds are hard materials ($H_V > 10$ GPa) and the hardness order is $\beta-Ti_3GaN_2 < \alpha-Ti_3GaN_2 < Ti_2GaN < \beta-Ti_4GaN_3 < \alpha-Ti_4GaN_3$. As an important result, the most stable structure ($\alpha-Ti_4GaN_3$) has the highest hardness.

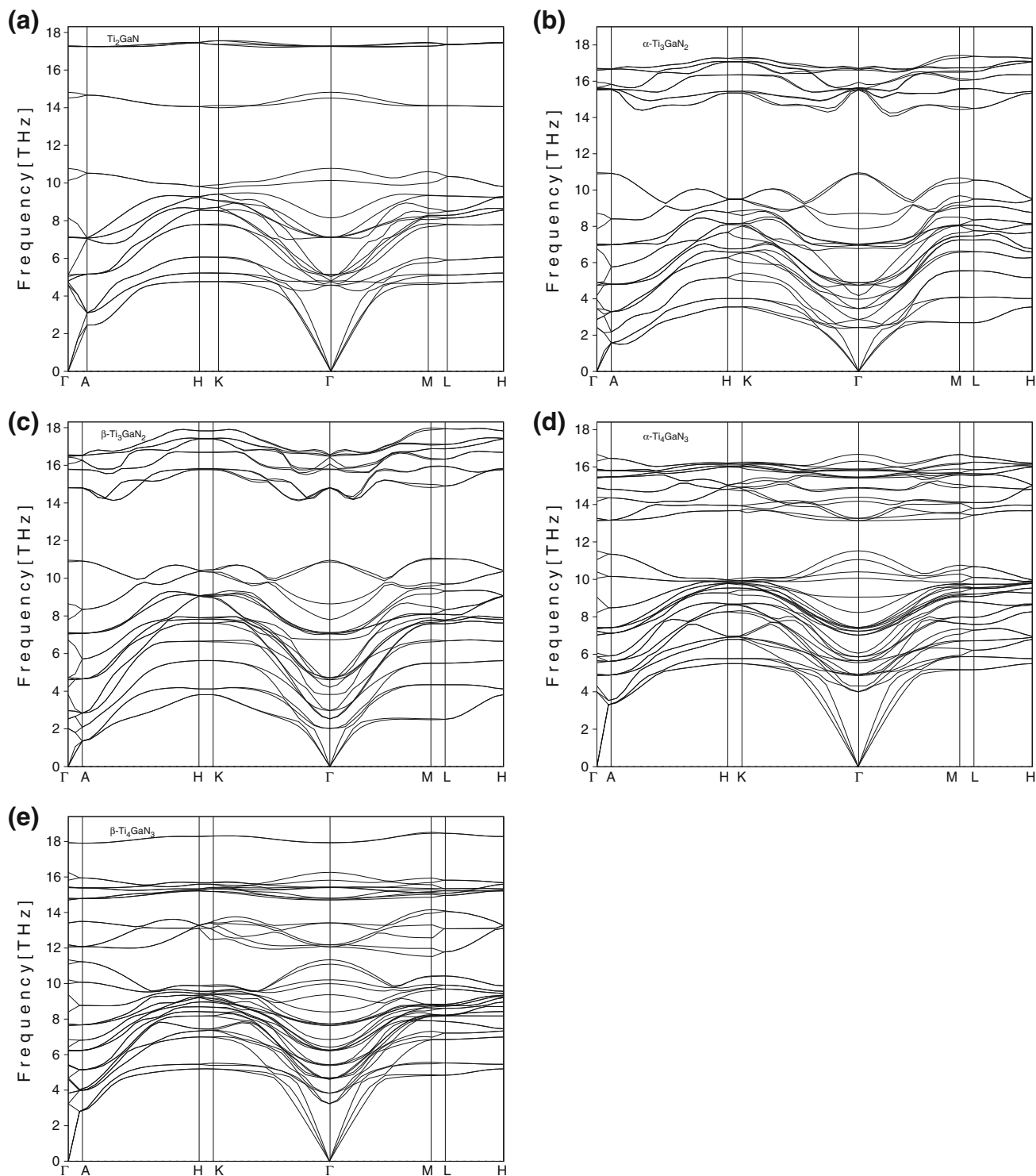


Fig. 3. Calculated phonon dispersion curves of $Ti_{n+1}GaN_n$ ($n = 1, 2$, and 3) compounds.

THERMODYNAMIC PROPERTIES

The calculated phonon dispersion can be used to compute energy (E), entropy (S), free energy (F),

and heat capacity (C_v) as functions of temperature on 0–1000 K range. The quantities were calculated by the following relations^{32,33},

Table III. The calculated sound velocity (V in m/s) using the acoustic phonon branches for $Ti_{n+1}GaN_n$ compounds

	V_{LA} [100]	V_{TA} [100]	V_{LA} [110]	V_{TA} [110]
Ti_2GaN	7243	4409	4740	6922
$\alpha-Ti_3GaN_2$	6295	3942	4001	6017
$\beta-Ti_3GaN_2$	5825	3626	3285	5699
$\alpha-Ti_4GaN_3$	6622	4044	4044	6218
$\beta-Ti_4GaN_3$	6060	3733	3327	5938

Table IV. The calculated Elastic constants (C_{ij} , in GPa) for $Ti_{n+1}GaN_n$ compounds

	C_{11}	C_{12}	C_{13}	C_{33}	C_{44}
Ti_2GaN					
Present (stress-strain)	299.90	77.28	91.83	275.80	126.22
Present (slope technique)	297.41	77.00	115.57	271.64	127.34
Theory ^a	297 ^a	83 ^a	91 ^a	273 ^a	119 ^a
Theory ^b	296 ^b	84 ^b	92 ^b	275 ^b	119 ^b
$\alpha-Ti_3GaN_2$					
Present (stress-strain)	337.49	82.80	123.64	308.25	133.98
Present (slope technique)	336.43	72.50	122.93	307.34	135.90
$\beta-Ti_3GaN_2$					
Present (stress-strain)	344.21	91.85	99.73	334.66	110.46
Present (slope technique)	342.74	77.06	100.70	328.08	109.04
$\alpha-Ti_4GaN_3$					
Present (stress-strain)	401.37	103.38	108.72	357.78	154.70
Present (slope technique)	399.95	101.62	131.20	352.59	149.13
$\beta-Ti_4GaN_3$					
Present (stress-strain)	400.00	100.49	101.01	389.62	117.96
Present (slope technique)	398.14	96.08	110.84	382.21	119.96

^aRef. 2. ^bRef. 7.**Table V. The calculated bulk modulus (B , in GPa), Shear Modulus (G , in GPa), Young's modulus (E in GPa), Poisson's ratio (ν), and Hardness (H_V , in GPa) for $Ti_{n+1}GaN_n$ compounds**

	B	G	E	B/G	ν	H_V
Ti_2GaN	155.25	113.04	272.90	1.37	0.21	18.93
	155 ^a	109 ^a	266 ^a	1.42 ^a	0.21 ^a	
	156 ^b	108 ^b	264 ^b	1.44 ^b	0.22 ^b	
$\alpha-Ti_3GaN_2$	182.57	121.25	297.82	1.51	0.23	17.51
$\beta-Ti_3GaN_2$	178.44	118.02	290.10	1.51	0.23	17.09
$\alpha-Ti_4GaN_3$	200.03	147.34	354.90	1.36	0.20	22.95
$\beta-Ti_4GaN_3$	199.38	135.41	331.23	1.47	0.22	19.46

^aRef. 2. ^bRef. 6.

$$E(T) = E_{wt} + E_{zp} + \int \frac{\hbar w}{\exp(\frac{\hbar w}{kT}) - 1} F(w) dw \quad (4) \quad F(T) = E_{tot} + E_{zp} + kT \int F(w) \ln \left[1 - \exp\left(-\frac{\hbar w}{kT}\right) \right] dw$$

$$S(T) = k \left\{ \int \frac{\hbar w}{\exp(\frac{\hbar w}{kT}) - 1} F(w) dw \right. \quad (5) \quad (6)$$

$$\left. - \int F(w) \left[1 - \exp\left(-\frac{\hbar w}{kT}\right) \right] dw \right\} \quad C_v(T) = k \int \frac{(\frac{\hbar w}{kT})^2 \exp(\frac{\hbar w}{kT})}{[\exp(\frac{\hbar w}{kT}) - 1]^2} F(w) dw \quad (7)$$

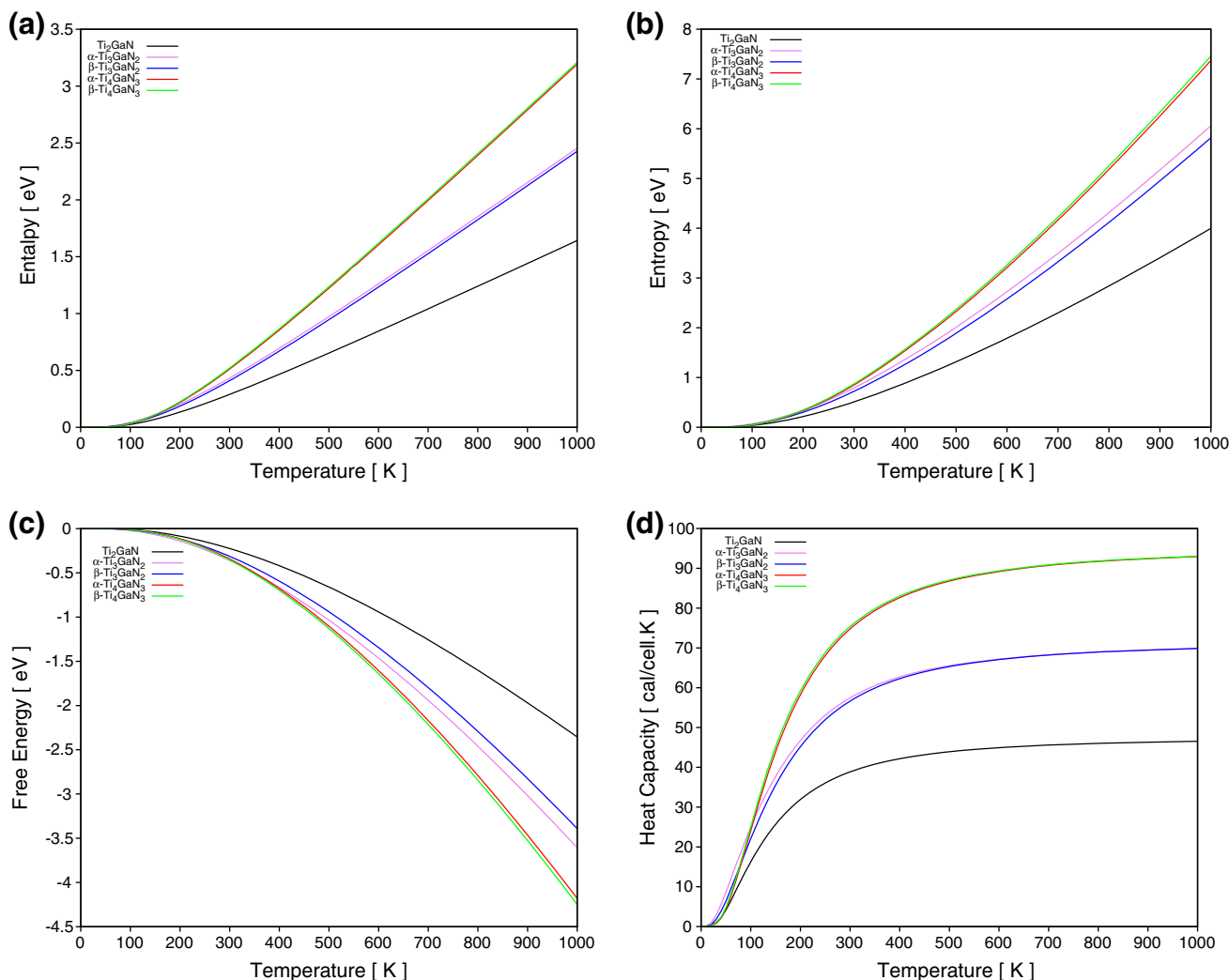


Fig. 4. Calculated thermodynamic properties of $\text{Ti}_{n+1}\text{GaN}_n$ ($n = 1, 2, \text{ and } 3$) compounds.

where E_{zp} is the zero-point energy, k is the Boltzmann's constant, \hbar is the Planck's constant and $F(\omega)$ is the phonon density of states. All energy-related properties including the enthalpy, entropy, and free energy for $\text{Ti}_{n+1}\text{GaN}_n$ are plotted in Fig. 4a–c, respectively. In an ensemble where the sample volume and temperature are independent variables, the relevant potential is the Helmholtz free energy, $F = E - T.S$. So, the entropy is presented as a $T.S$ product to allow comparison with the enthalpy and Helmholtz free energy.

Above 200 K, the free energy decreases gradually with increasing temperature and the value of the entropy, which is multiplied by the temperature, increases rapidly as the temperature increases, resulting in an almost linear relationship between enthalpy and temperature. The rate of change of entropy, enthalpy, and free energy with increasing temperature can be sorted from the highest to lowest as $\beta\text{-Ti}_4\text{GaN}_3$, $\alpha\text{-Ti}_4\text{GaN}_3$, $\alpha\text{-Ti}_3\text{GaN}_2$, $\beta\text{-Ti}_3\text{GaN}_2$, Ti_2GaN , respectively.

From Fig. 4d, C_v increases rapidly with temperature below 400 K, whereas the increase is slower above 400 K. In addition, the heat capacity approaches a constant known as the Dulong–Petit limit at higher temperatures.

CONCLUSIONS

First-principles calculations were performed to investigate the structural, electronic, mechanical, and dynamic properties of $\text{Ti}_{n+1}\text{GaN}_n$ compounds, among which $\alpha\text{-Ti}_4\text{GaN}_3$ was found to be energetically the most stable. The calculated elastic constants showed that these compounds are mechanically stable. The polycrystalline elastic parameters have been further calculated within the scheme of Voigt–Reuss–Hill (VRH) approximation. These phases are brittle in nature with respect to the B/G and hard materials. The computed density of states of $\text{Ti}_{n+1}\text{GaN}_n$ compounds reveals a metallic character. Phonon calculations confirm the dynamical stability of the studied phases. We believe that

our results can serve as a prediction for future investigations.

ACKNOWLEDGEMENTS

This work was partly supported by the State Planning Organization of Turkey under Grant No. 2011K120290. Some of the calculations were performed in the high performance computing center (HPCC) at Gazi University.

REFERENCES

1. M.W. Barsoum, *Prog. Solid State Chem.* 28, 201 (2000).
2. Z.J. Yang, J. Li, R.F. Linghu, X.L. Cheng, and X.D. Yang, *J. Alloys Comp.* 574, 573 (2013).
3. X. Hea, Y. Bai, Y. Li, C. Zhu, and M. Li, *Solid State Commun.* 149, 564 (2009).
4. M.W. Barsoum, *Physical Properties of the MAX Phases, Encyclopedia of Materials: Science and Technology* (Amsterdam: Elsevier, 2006).
5. M. Dahlgvist, B. Alling, and J. Rosén, *Phys. Rev. B* 81, 220102 (2010).
6. V.J. Keast, S. Harris, and D.K. Smith, *Phys. Rev. B* 80, 214113 (2009).
7. A. Bouhemadou, *Solid State Sci.* 11, 1875 (2009).
8. B. Manoun, S. Kulkarni, N. Pathak, S.K. Saxena, S. Amini, and M.W. Barsoum, *J. Alloys Comp.* 505, 328 (2010).
9. I.R. Shein and A.L. Ivanovskii, *Comput. Mater. Sci.* 65, 104 (2012).
10. P. Eklund, M. Beckers, U. Jansson, H. Högberg, and L. Hultman, *Thin Solid Films* 518, 1851 (2010).
11. M.D. Segall, P.J.D. Lindan, M.J. Probert, C.J. Pickard, P.J. Hasnip, S.J. Clark, and M.C. Payne, *J. Phys.* 14, 2717 (2002).
12. J.P. Perdew and Y. Wang, *Phys. Rev. B* 45, 13244 (1992).
13. D.R. Hamann, M. Schlüter, and C. Chiang, *Phys. Rev. Lett.* 43, 1494 (1979).
14. N. Troullier and J.L. Martins, *Phys. Rev. B* 43, 1993 (1991).
15. H.J. Monkhorst and J.D. Pack, *Phys. Rev. B* 13, 5188 (1976).
16. T.H. Fischer and J. Almlof, *J. Phys. Chem.* 96, 9768 (1992).
17. J.H. Xu, T. Oguchi, and A.J. Freeman, *Phys. Rev. B* 35, 6940 (1987).
18. J.H. Xu and A.J. Freeman, *Phys. Rev. B* 40, 11927 (1989).
19. B. Montanari and N.M. Harrison, *Chem. Phys. Lett.* 364, 528 (2002).
20. E. Deligoz, K. Colakoglu, and Y.O. Ciftci, *J. Phys. Chem. Solids* 68, 482 (2007).
21. B.A. Auld, *Acoustic Fields and Waves in Solid*, 1st ed. (New York: John Wiley & Sons, 1973), 391.
22. N.W. Ashcroft and N.D. Mermin, *Solid State Physics*, 1st ed. (Philadelphia: Saunders, 1976), 447.
23. J.F. Nye, *Physical Properties of Crystals*, 1st ed. (Oxford: Clarendon, 1957), 148.
24. Z.J. Wu, E.J. Zhao, H.P. Xiang, X.F. Hao, X.J. Liu, and J. Meng, *Phys. Rev. B* 76, 054115 (2007).
25. P. Rong-Kai, M. Li, B. Nan, W. Ming-Hui, L. Peng-Bo, T. Bi-Yu, P. Li-Ming, and D. Wen-Jiang, *Phys. Scr.* 87, 015601 (2013).
26. R. Hill, *Proc. Phys. Soc. Lond. A* 65, 349 (1952).
27. M. Rajagopalan, S.P. Kumar, and R. Anuthama, *Phys. B* 405, 1817 (2010).
28. N. Korozlu, K. Colakoglu, E. Deligoz, and S. Aydin, *J. Alloys Comp.* 546, 157 (2013).
29. S.F. Pugh, *Phil. Mag. Ser.* 45, 823 (1954).
30. V.V. Bannikov, I.R. Shein, and A.L. Ivanovskii, *Phys. Stat. Sol. (RRL)* 3, 89 (2007).
31. X.Q. Chen, H. Niu, D. Li, and Y. Li, *Intermetallics* 19, 1275 (2011).
32. S.D. Gironcoli, A.D. Corso, and P. Giannozzi, *Rev. Mod. Phys.* 73, 515 (2001).
33. P.K. Jha, *Phys. Rev. B* 72, 214502 (2005).